

Searches for BSM physics in dilepton, multilepton and lepton+MET final states at CMS

L. Benato^{1,2,a} on behalf of CMS Collaboration

¹Università degli Studi di Padova

²INFN sezione di Padova

Abstract. Numerous new physics models, e.g., theories with extra dimensions and various gauge-group extensions of the standard model, predict the existence of new particles decaying to dilepton, multilepton, and lepton+MET final states. This talk presents the recent results from searches for new physics in the leptonic final states at CMS.

1 Introduction

Many Beyond Standard Model (BSM) physics models foresee the appearance of particles at high mass range, decaying into dilepton, multilepton and lepton + neutrino final states. Leptons considered in these searches are electrons and muons; neutrinos are revealed as missing transverse energy in the detector (E_T^{miss}). The leptonic final states are historically channels of discovery and precision measurements, because they show very clean signatures; dealing with high energetic leptons coming from heavy resonances, however, implies careful studies of the objects and their properties. Generally these models predict very small branching ratio for leptonic decays: as a consequence, the statistical uncertainties dominate, so it is necessary to accurately evaluate the backgrounds. Results obtained from the LHC Run 2 data collected in 2015 by the CMS experiment [1] are presented: going up to $\sqrt{s} = 13$ TeV makes the parton luminosities of processes $q\bar{q} \rightarrow X$ increase substantially, especially at high mass region, improving the previous limits set on these models by LHC Run 1 data. [2]-[5]

2 CMS detector

CMS is a multi-purpose experiment composed of many sub-systems enclosed in a superconducting magnet. Informations coming from different sub-detectors can be used together to improve the energy and momentum determination of the particles involved.

3 High energy objects

As a general approach, isolation requirements are applied to charged leptons, in order to reduce backgrounds coming from objects (mainly jets) misidentified as leptons. A lepton is isolated if the ratio of the energy deposits around its track divided by its transverse momentum (p_T) is below a certain threshold.

^ae-mail: lisa.benato@cern.ch

3.1 Muons

Muons are challenging objects to reconstruct at high energy values: in these conditions, their trajectory in the magnetic field is almost straight, complicating the determination of their p_T and charge. The precision of their p_T measurement, furthermore, is strongly influenced by the alignment of the external muon gas detectors and the inner silicon tracker. In addition, high energetic muons radiate in the detector materials, causing a loss of resolution at increasing p_T . Many studies in this sense have been performed on the cosmic muons collected by CMS. Different high- p_T muon reconstruction algorithms have been exploited: they generally combine informations from muon chambers and tracker, in order to improve the identification efficiency as much as possible and to discard the segments in the muon chambers where radioactive phenomena occurred.

3.2 Electrons

Electrons are reconstructed using informations coming from all the sub-detectors. Dedicated selections for high- p_T electrons are applied in these analyses, in order to achieve the highest detection efficiency. Unlike muons, electron energy and p_T resolutions are approximatively constant at increasing energy.

3.3 E_T^{miss}

The experimental signature of the presence of a non-interacting particle, the neutrino, is represented by the missing transverse energy, E_T^{miss} . The quantity $p_T^{\vec{miss}}$ is defined as the negative sum $-\Sigma p_T^{\vec{}}$ of all reconstructed particles; E_T^{miss} is the modulus of $p_T^{\vec{miss}}$. Its magnitude is influenced by all the other objects, including jets and their corrections.

4 Heavy spin-1 BSM bosons searches in dilepton and lepton plus E_T^{miss} final states

A common feature of models admitting new physics consists into enlarging the Standard Model gauge symmetry group, $SU(3) \times SU(2) \times U(1)$, into a larger one that, once broken into the SM group, will result into new residual groups: new spin-1 heavy bosons are expected to appear. The most naïf extension is the Sequential Standard Model [6], in which two W'_{SSM} and a Z'_{SSM} are expected to be the heavy replicas of W and Z bosons, with the same couplings to leptons as their standard model partners. More exotic spin-1 heavy bosons predicted by super string inspired models, like a Z'_ψ coming from $E(6)$ breaking [7]-[8], are searched for in the following analysis.

4.1 $Z' \rightarrow \ell^+ \ell^-$ [9]

The analysis strategy consists into reconstructing the invariant mass of the heaviest $\ell^+ \ell^-$ pair, after applying adequate selections to all the leptonic candidates, in order to suppress the background contributions in favour of the expected signal. The main source of irreducible background events is represented by the Drell-Yan process, $Z/\gamma^* \rightarrow \ell^+ \ell^-$, that is well estimated by Monte Carlo simulated events. Monte Carlo simulations also work for the second category of backgrounds, which contains real prompt leptons coming from processes like $t\bar{t}$, tW , WW , WZ , ZZ ; these predictions are validated on data in $e\mu$ control region, where no signal is expected. Non-prompt backgrounds, that are objects (mainly jets) misidentified as leptons, are predicted via data-driven methods. Cosmic muons

are suppressed applying a cut on the impact parameter with respect to the primary vertex of the hard interaction and on the 3D angle between the muons.

The observed and the predicted SM backgrounds invariant mass spectra are shown in Fig. 1 for muons (left) and electrons (right). No discrepancy is seen among the two distributions. The highest mass event is observed in the electron channel, and it is located at 2.9 TeV. The expected number of events above 2.8 TeV is $0.036 \pm 0.009 ee$, 1 is seen. The local p-value for the null-hypothesis calculated as the Poisson probability to observe at least one event in the electron channel above 2.8 TeV is 0.036.

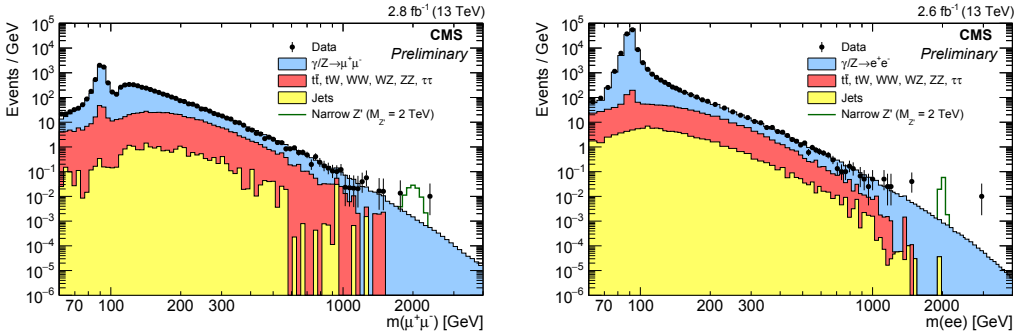


Figure 1. $Z' \rightarrow \ell^+ \ell^-$ search. The invariant mass spectrum of $\mu^+ \mu^-$ (left) and $e^+ e^-$ (right) events. The points with error bars represent the data. The histograms represent the expectations from standard model processes: Drell-Yan, other sources of prompt leptons ($t\bar{t}$, tW , WW , WZ , ZZ , $Z \rightarrow \tau\tau$), and non-prompt backgrounds. The green curve represents an hypothetical Z' of mass 2 TeV.

Limits at 95% confidence level on the ratio between the cross-section times branching ratio for the Z' divided by the same quantity for the Z are extracted:

$$\frac{\sigma(pp \rightarrow Z' + X \rightarrow \ell\ell + X)}{\sigma(pp \rightarrow Z/\gamma^* + X \rightarrow \ell\ell + X)}$$

The ratio cancels the luminosity uncertainties. A Bayesian unbinned likelihood approach is applied; the likelihood is integrated using the Metropolis-Hastings algorithm. The main uncertainties related to signal efficiency and cross-section are due to lepton identification (6% for electrons, 7% for muons). The background uncertainty comes mainly from PDF uncertainties (up to 20% at 3 TeV). A mass scale uncertainty (1% for e , 3% for μ) is applied while combining the channels. The signal is modelled as the convolution of a Breit-Wigner and a Gaussian distribution, under the narrow width approximation: this means that only the on-shell region of the resonance is considered, because the interference is strongly model-dependent. In Fig. 2 (left), expected and observed limits for different signal widths are shown, ranging from 0%, to 0.6% of the expected resonance mass (as predicted by Z'_ψ), to 3% of the mass (as predicted by Z'_{SSM}), combining the e and μ channel. The final expected and observed limits for the combination of electron and muon channels under the hypothesis of a width of 0.6% are displayed in the right panel of Fig. 2. In Tab. 1, a more detailed summary of the mass limits for each channel and model is reported.

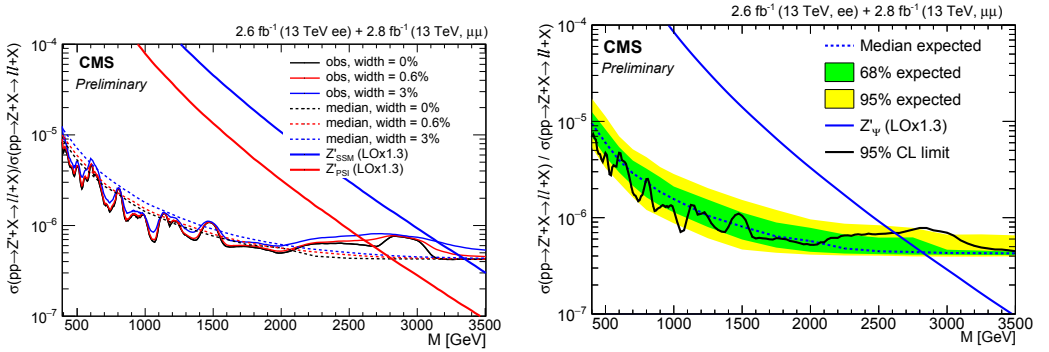


Figure 2. $Z' \rightarrow \ell^+ \ell^-$ search. Left: 95% confidence level observed and expected limits on the cross-section ratio for different resonance widths; they are obtained combining the electron and muon channels. Right: limits set at 95% confidence level for a Z' whose natural width is the 0.6% of its mass. The theoretical curves of the discussed models are included in the plots.

Table 1. $Z' \rightarrow \ell^+ \ell^-$ search. Observed limits on the mass of Z'_ψ and Z'_{SSM} for each channel and for the combination.

Channel	Z'_ψ	Z'_{SSM}
ee	2.40 TeV	2.75 TeV
$\mu\mu$	2.40 TeV	3.00 TeV
combination	2.60 TeV	3.15 TeV

4.2 $W' \rightarrow \ell\nu$ [10]

In this analysis, since a neutrino is expected in the final state, the discriminant variable is the transverse invariant mass, which takes into account only the transverse quantities:

$$M_T = \sqrt{2p_T^\ell E_T^{miss} \left(1 - \cos \left[\Delta\phi(\vec{p}_T^\ell, \vec{p}_T^{miss}) \right] \right)}.$$

In order to achieve a back-to-back topology between the lepton and the neutrino, a cut is applied on their azimuthal angles, $|\Delta\phi(\vec{p}_T^\ell, \vec{p}_T^{miss})| > 2.5$. A further selection, $0.4 < p_T/E_T^{miss} < 1.5$, allows to reject background contamination.

The dominant source of background is represented by the standard model $W \rightarrow \ell\nu$ process, and it is fully predicted by Monte Carlo simulations. Secondary backgrounds like Drell-Yan processes, $t\bar{t}$, single t , WW , WZ , ZZ are also taken from simulations. QCD multijet backgrounds are estimated from data. Cosmic muons contamination is suppressed with a cut on impact parameter with regards to the primary vertex, like in the previous analysis.

In Fig. 3, the transverse mass distributions are shown for muon (left) and electron (right) channel. Data and Monte Carlo spectra are in agreement.

Limits at 95% confidence level on cross-section $\sigma(pp \rightarrow W' + X \rightarrow \ell\nu + X)$ are extracted via the modified frequentist approach (CL_s method [11]-[12]). Limits are provided in a region over 1 TeV, where Run 2 data are more sensitive due to the increased center of mass energy and, consequently, increased cross-section for the considered process. The main uncertainties in the muon channel arise

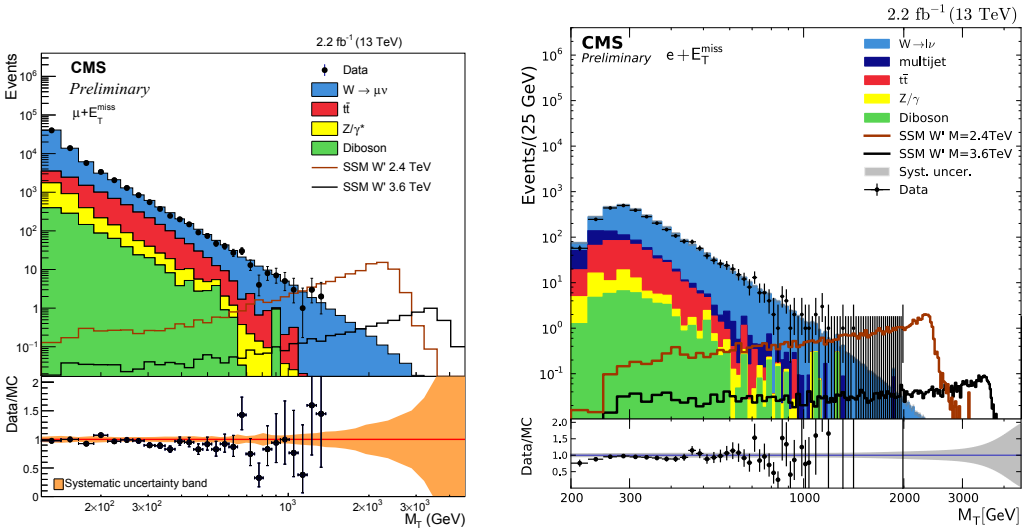


Figure 3. $W' \rightarrow \ell\nu$ search. The transverse mass spectrum of $\mu\nu$ (left) and $e\nu$ (right) events. The points with error bars represent the data. The histograms represent the expectations from standard model processes: W decays, other sources of prompt leptons (Z/γ^* , $t\bar{t}$, tW , WW , WZ , ZZ , $Z \rightarrow \tau\tau$), and non-prompt backgrounds. The dark orange and black curves represent two hypothetical W' of mass 2.4 and 3.6 TeV.

from the muon momentum scale and p_T resolution, that both propagate to E_T^{miss} , as pointed out in Sec. 3.1 and 3.3. The electron channel is mainly affected by PDF uncertainties, especially at high M_T .

The expected and observed limits for the cross-section obtained combining the two channels are shown in Fig. 4; the final limits on the W'_{SSM} mass for each channel are summarized in Tab. 2.

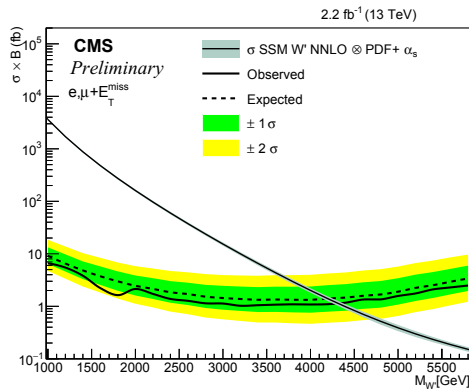


Figure 4. $W' \rightarrow \ell\nu$ search. 95% confidence level observed and expected limits on the cross-section compared to the theoretical curve predicted for a W'_{SSM} . Limits are obtained by combining the electron and muon channels.

Table 2. $W' \rightarrow \ell\nu$ search. Observed limits on the mass of a W'_{SSM} for each channel and for the combination.

Channel	W'_{SSM}
e	3.8 TeV
μ	4.0 TeV
combination	4.4 TeV

5 Seesaw type-III mechanism search in multilepton final states [13]

A remarkable puzzle left unsolved by the Standard Model is related to neutrino masses. An appealing possibility is represented by the seesaw mechanism: it introduces new heavy particles coupling to leptons and to Higgs doublets, accounting for both the neutrino masses and their smallness (six or more orders of magnitude smaller than that of the electron). In particular, in the type-III seesaw model [14], the neutrino is considered a Majorana particle whose mass arises via the mediation of a massive fermionic triplet, composed by the heavy Dirac charged Σ^\pm , and the heavy Majorana neutral Σ^0 . In high energy proton-proton collisions, the heavy fermions may be produced in pairs through electroweak interactions. In this search, a final state with at least three charged leptons (electrons or muons) is considered: the heavy triplet can decay into leptons via electroweak or Higgs bosons. In Fig. 5, one of the 27 possible decay modes is pictured. The decay rate of a Σ to a particular flavour ℓ is proportional to $\frac{V_\ell}{\sqrt{|V_e|^2+|V_\mu|^2+|V_\tau|^2}}$, where each V_ℓ represents the coupling of the heavy fermion to the considered leptonic flavour. In the flavour democratic scenario, V_ℓ is the same for e, μ and τ .

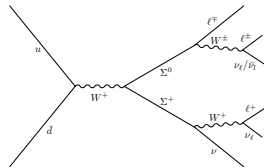


Figure 5. Seesaw type-III search. Feynman diagram example of the fermion Σ production and decay in leptonic final states in the context of the type-III seesaw model.

The analysis strategy is based on grouping the final states in categories, depending on the number of reconstructed leptons, the number of opposite sign same flavour pairs (OSSF), zero, one or two, and on the invariant mass of the pair, on or under-above the nominal mass of the Z boson. A promising cut that has been studied to reject backgrounds is the scalar sum of the p_T of all the considered leptons, L_T , added to E_T^{miss} , requiring $L_T + E_T^{miss} > 350$ GeV: this guarantees high efficiency for both channels involving decays where the momentum is carried by leptons, like $\Sigma^\pm \rightarrow Z\ell^\pm \rightarrow \ell^\pm\ell'^+\ell'^-$, and decays where there is a large amount of missing transverse energy, like $\Sigma^0 \rightarrow H\nu \rightarrow WW\nu$. Considering the most significant channels in terms of expected signal given the luminosity, the analysis consists in keeping 4 distributions, depending on the lepton properties: 3 leptons without an OSSF pair, 3 leptons with one OSSF pair on-Z, 3 leptons with one OSSF pair above-Z, and 4 leptons with at least one OSSF pair. In left Fig.6, the spectrum of $L_T + E_T^{miss}$ for the category 1 OSSF pair, 3 leptons, $m_{\ell^+\ell^-}$ above-Z is displayed, whilst in right Fig.6 there is the spectrum for the category where there is at least 1 OSSF, 4 leptons, no requirements on $m_{\ell^+\ell^-}$: it is noticeable that the statistics is very low. Data and Monte Carlo spectra are in agreement.

Backgrounds strongly depend on the categories considered. 51% of the total expected background is represented by the standard model decay $WZ \rightarrow \ell\ell\ell$, that is predicted by Monte Carlo simulations

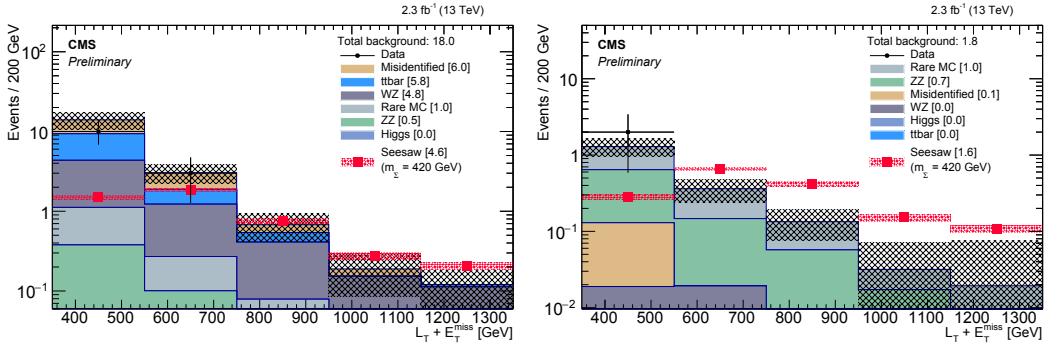


Figure 6. *Seesaw type-III search.* Left: spectrum of $L_T + E_T^{miss}$ for the category 1 OSSF pair, 3 leptons, $m_{\ell^+\ell^-}$ -above-Z. Right: spectrum of $L_T + E_T^{miss}$ for the category at least 1 OSSF pair, 4 leptons, no requirements on $m_{\ell^+\ell^-}$. The points with error bars represent the data. The histograms represent the expectations from standard model processes: WZ, $t\bar{t}$, ZZ, Higgs decays, rare processes and misidentified leptons. The red points represent a hypothetical Σ of mass 420 GeV.

and validated on data. The kinematics of the leptonic $t\bar{t}$ decays, with a misidentified lepton from a b-jet, is predicted by Monte Carlo samples; the misidentification rate, instead, is measured in data control region. $Z \rightarrow \ell\ell$ plus a misidentified lepton in jet is predicted with a data-driven method. Other processes, like $ZZ \rightarrow 4\ell$, $t\bar{t}Z$, $t\bar{t}W$, $H \rightarrow 4\ell$, are evaluated via Monte Carlo simulations.

Limits at 95% confidence level on the cross-section sum for the production of seesaw heavy fermionic pairs $\Sigma^0\Sigma^+$, $\Sigma^0\Sigma^-$, $\Sigma^+\Sigma^-$ and on their mass are extracted with the asymptotic CL_s method, under the assumptions of a degenerate m_Σ , and of the flavour democratic scenario, where $V_e = V_\mu = V_\tau = 10^{-6}$. They are reported in Fig. 7 and in Tab. 3. The p-value for the observation in all the considered channels, assuming there is no new physics, is 0.93. The uncertainties are strongly dominated by statistics; systematic uncertainties are small and mainly due to PDF and to renormalization and factorization uncertainties related to E_T^{miss} range in the dominant WZ background.

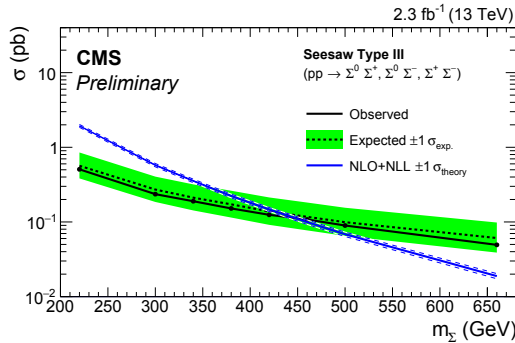


Figure 7. *Seesaw type-III search.* Expected and observed limits at 95% confidence level on the cross-section sum for the production of seesaw heavy fermion pairs $\Sigma^0\Sigma^+$, $\Sigma^0\Sigma^-$, $\Sigma^+\Sigma^-$. The theoretical curve of the discussed model is included in the plot.

Table 3. *Seesaw type-III search.* Observed limit on the mass of the seesaw type-III mediators.

Channel	m_Σ
combination	440 GeV

6 Quantum black holes search in $e\mu$ final state [15]

Many extensions of the Standard Model predict the existence of heavy resonances decaying into lepton flavour violating final states, like $e\mu$. If a fundamental Planck scale could be observable at TeV, the production of microscopic black holes decaying into couples of particles should be possible at the LHC, once the production mass threshold M_{th} is reached. In particular, in the considered models [16]-[17], quantum black holes (QBH) are spin-0, colourless, neutral particles, and lepton flavour violation is allowed. A search in this sense has been performed; the interpretation of the results depends on the number of extra-dimensions n involved: for $n = 1$, a Randall-Sundrum scenario is considered, while for $n \geq 2$, we lay in the ADD scenarios.

The analysis strategy consists in reconstructing the invariant mass distribution of the $e\mu$ pairs, without requiring to the leading leptons to be opposite sign, in order to avoid an efficiency loss due to the wrong assignment of the electron charge in high energy range. The misidentification of the objects involved is reduced by rejecting all the electrons close (in a cone $\Delta R < 0.1$) to muons that produce bremsstrahlung. In left Fig.8, the invariant mass spectrum of the $e\mu$ pairs is presented; the right plot is the cumulative distribution of the previous one. Data and Monte Carlo spectra are in agreement.

The backgrounds contributing to the final state can be divided into two categories: the first comprises events with at least two prompt, isolated leptons; the second includes jets and photons misidentified as isolated leptons or jets with non-prompt leptons coming from heavy-flavour decays. In the former category, processes like $t\bar{t}$, WW , WZ , ZZ , single t , Drell-Yan are included, and they are estimated from Monte Carlo samples; in the latter category, the dominant contribution is represented by $W + jets$ processes, and all these backgrounds are predicted with data-driven methods.

An upper limit at 95% confidence level on the cross-section times branching ratio is determined using a binned likelihood Bayesian approach, and it is shown in Fig. 9. The non-resonant signal is modelled as a broad shape smeared by the detector resolution, with a sharper edge at M_{th} . The uncertainties, entering the limit extraction as nuisance parameters, are modelled with log-normal distributions. The uncertainty on the muon momentum scale (10% per TeV) propagates to an uncertainty on the background yield of 30% at 3 TeV. The dominant uncertainty in the background yield prediction is due to the uncertainty on the shape of the $e\mu$ distribution in the $t\bar{t}$ background, that ranges up to 31% at 2 TeV. The final limits on the threshold mass of the QBH are reported in Tab. 4, as a function of the extra-dimensions considered in the theoretical model.

Table 4. *Quantum black holes in $e\mu$ search.* Observed limits on the production mass threshold of a quantum black hole, considering a different number of extra-dimensions involved, from $n = 1$ (Randall-Sundrum scenario), up to $n = 6$ (ADD scenarios).

n	M_{th}
1 (RS)	2.5 TeV
4 (ADD)	4.2 TeV
5 (ADD)	4.3 TeV
6 (ADD)	4.5 TeV

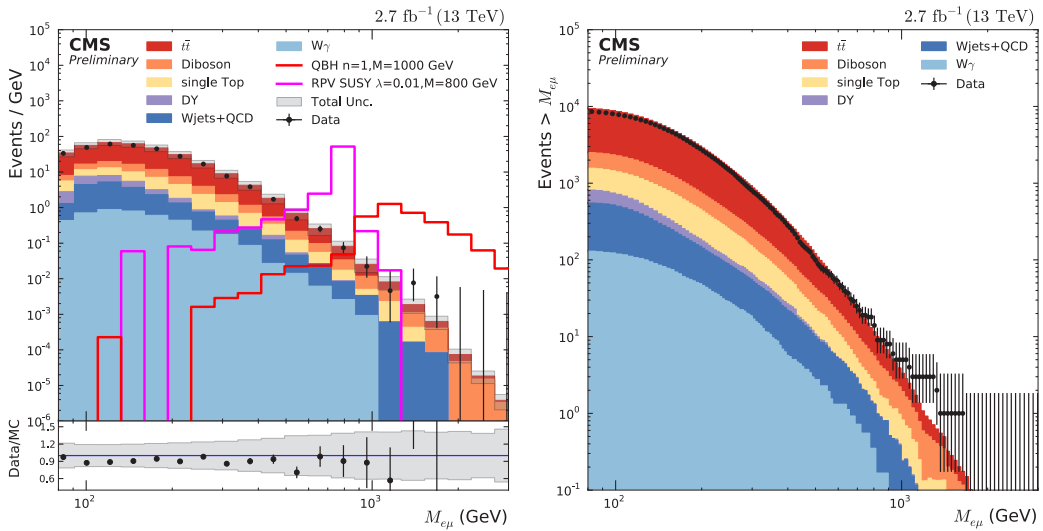


Figure 8. *Quantum black holes in $e\mu$ search.* Left: invariant mass spectrum of the $e\mu$ pairs. Right: cumulative distribution of the invariant mass spectrum of the $e\mu$ pairs. The points with error bars represent the data. The histograms represent the expectations from standard model processes: W +jets, $W\gamma$, $t\bar{t}$, WW , WZ , ZZ , single t , Drell-Yan. The red curve in the left plot represents an hypothetical QBH of mass 1 TeV in a Randall-Sundrum scenario ($n = 1$).

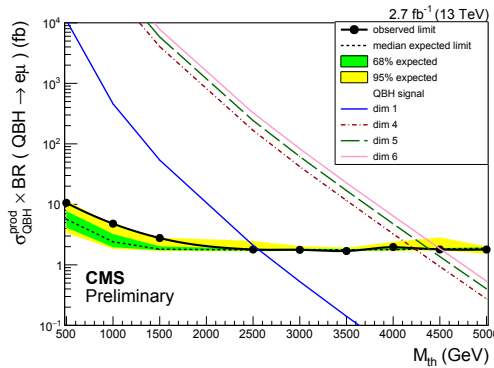


Figure 9. *Quantum black holes in $e\mu$ search.* Expected and observed limits at 95% confidence level on the cross-section times branching ratio for the quantum black hole production. The theoretical curves of the discussed models are included in the plot.

7 Conclusions

The LHC collider is facing its "search era": searching for heavy resonances predicted by BSM models that decay into leptons and neutrinos is considered a high-priority task nowadays. Many searches have been performed during Run 2 in 2015 by the CMS collaboration: the increased \sqrt{s} allowed improvements with regards to Run 1 analyses, pushing the exclusion limits to higher masses of the

considered states. These searches are being repeated in 2016 data: more luminosity is expected and more interesting results are coming soon.

References

- [1] CMS Collaboration, “The CMS experiment at the CERN LHC”, *JINST* **3**, S08004 (2008)
- [2] CMS Collaboration, “Search for physics beyond the standard model in dilepton mass spectra in proton-proton collisions at $\sqrt{s} = 8$ TeV”, *JHEP* **04**, 025 (2015)
- [3] CMS Collaboration, “Search for physics beyond the standard model in final states with a lepton and missing transverse energy in proton-proton collisions at $\sqrt{s} = 8$ TeV”, *Phys. Rev.* **D91**, 092005 (2015)
- [4] CMS Collaboration, “Search for heavy lepton partners of neutrinos in proton-proton collisions in the context of the type III seesaw mechanism”, *Phys. Lett.* **D718**, 348 (2012)
- [5] CMS Collaboration, “Search for lepton flavour violating decays of heavy resonances and quantum black holes to an e-mu pair in proton-proton collisions at $\sqrt{s} = 8$ TeV”, *Eur. Phys. J.* **C76**, 317 (2016)
- [6] G. Altarelli, B. Mele, and M. Ruiz-Altaba, “Searching for new heavy vector bosons in $p\bar{p}$ colliders”, *Z. Phys.* **C45**, 109 (1989)
- [7] A. Leike, “The phenomenology of extra neutral gauge bosons”, *Phys. Rept.* **317**, 143 (1999)
- [8] J. L. Hewett and T. G. Rizzo, “Low-energy phenomenology of superstring-inspired E6 models”, *Physics Reports* **183**, 193 (1989)
- [9] CMS Collaboration, “Search for a Narrow Resonance Produced in 13 TeV pp collisions decaying to electron pair or muon pair final states”, CMS Physics Analysis Summary CMS-PAS-EXO-15-005, 2015
- [10] CMS Collaboration, “Search for SSM W' production, in the lepton+MET final state at a center-of-mass energy of 13 TeV”, CMS Physics Analysis Summary CMS-PAS-EXO-15-006, 2015
- [11] A. L. Read, “Presentation of search results: the CL_s technique”, *J. Phys. G: Nucl. Part. Phys.* **28**, 2693 (2002)
- [12] T. Junk, “Confidence level computation for combining searches with small statistics”, *Nucl. Instrum. Meth.* **A434**, 435 - 443 (1999)
- [13] CMS Collaboration, “Search for type-III seesaw heavy fermions with multilepton final states using 2.3 fb⁻¹ of $\sqrt{s} = 13$ TeV proton-proton collision data”, CMS Physics Analysis Summary CMS-PAS-EXO-16-002, 2016
- [14] R. Foot, H. Lew, X. He, and G. Joshi, “See-saw neutrino masses induced by a triplet of leptons”, *Z. Phys.* **C44**, (1989)
- [15] CMS Collaboration, “Search for high-mass resonances and quantum black holes in the $e\mu$ final state in proton-proton collisions at $\sqrt{s} = 13$ TeV”, CMS Physics Analysis Summary CMS-PAS-EXO-16-001, 2016
- [16] P. Meade and L. Randall, “Black Holes and Quantum Gravity at the LHC”, *JHEP* **05**, 003 (2008)
- [17] X. Calmet, W. Gong, and S. D. H. Hsu, “Colorful quantum black holes at the LHC”, *Phys. Lett.* **B668**, 20 - 23 (2008)